Boundary Effect on Diffusiophoresis: Spherical Particle in a Spherical Cavity

ARTICLE *in* LANGMUIR · FEBRUARY 2009

Impact Factor: 4.46 · DOI: 10.1021/la803334a · Source: PubMed

3 AUTHORS, INCLUDING:

Wei-Lun Hsu
The University of Tokyo
17 PUBLICATIONS **128** CITATIONS

SEE PROFILE

Boundary Effect on Diffusiophoresis: Spherical Particle in a Spherical Cavity

Jyh-Ping Hsu,* Wei-Lun Hsu, and Zheng-Syun Chen

Department of Chemical Engineering; National Taiwan University, Taipei, Taiwan 10617

Received October 8, 2008. Revised Manuscript Received November 25, 2008

The boundary effect on the diffusiophoretic behavior of a particle is analyzed theoretically by considering the diffusiophoresis of a charged sphere under arbitrary surface potential and double-layer thickness at an arbitrary position in an uncharged spherical cavity. We show that the phenomenon under consideration is governed by double-layer relaxation, chemiosmotic/diffusioosmotic flow, and two types of competing double-layer polarization. The presence of the cavity has a profound influence on the diffusiophoretic behavior of the particle, especially when the surface potential is high. For instance, the scaled diffusiophoretic velocity of the particle has a local maximum as the position of the particle varies; it may have a local maximum and local minimum as the thickness of the double-layer varies. The significance of the effect of double-layer relaxation depends upon the level of surface potential and magnitude of the electric Peclet number.

Introduction

Electrophoresis, one of the electrokinetic phenomena, has been analyzed and applied to various fields of both fundamental and practical significance.[1] Although the principle of electrophoresis is straightforward, namely, the driven of a charged entity by an applied electric field, several problems are present in practice. These include, for example, the boundary effect, the concentration effect, and the possible presence of electroosmotic flow. Another potential problem is the Joule heating effect arising from application of the external electric field. The increase in the temperature due to this effect may yield variations in the physicochemical properties of an electrophoresis system, thereby having a negative impact on electrophoresis.[2,3] One of the alternative methods to avoid the Joule heating effect is to replace the applied electric field by a concentration gradient, the diffusiophoresis, which was introduced by Deryagin et al.,[4,5] where both ionic and nonionic solutions were considered. Diffusiophoresis has been applied in particle separation[6] and latex particle coating processes.[7,8] For nonionic solutions a particle is driven by the van der Waals and dipole forces.[9−11] The direction of particle migration depends on the interaction force between the solute molecules and the particle. If the interaction force is attractive, the particle migrates toward the direction where the concentration of solute increases, and if it is repulsive, the particle migrates toward the opposite direction. For ionic solutions two major driving forces need be considered. The first driving force arises from the electric field established by the electrolyte concentration gradient on account of the difference of ionic diffusivities. Diffusion of high-mobility ions is decelerated due to the electrostatic force arising from the presence of low-mobility ions. On the other hand, diffusion of low-mobility ions is accelerated due to the presence of the high-mobility ions. That is, the difference in the ionic mobilities yields a background electric field, usually called electrophoresis, the intensity of which is measured by the relative diffusivity of ions. The second driving force is due to the effect of double-layer polarization caused solely by the imposed concentration gradient (neglecting the difference in ionic mobilities), usually called chemiphoresis.[12,13] Duhkin and Deryagin[14] suggested that because the diffusion layer on the high-concentration side of a particle is thinner than that on the low-concentration side the particle migrates toward the high-concentration side. Although this mechanism is applicable to many cases, exceptions were observed experimentally[15] and predicted theoretically[16] under conditions where the surface potential of a particle is sufficiently high. Assuming a thin double layer, Pawar et al.[17] were able to show that if the surface potential of a particle is high it migrates toward its low-concentration side in KCl solution. They pointed out that due to the electrostatic repulsive force coions accumulated in the region next to the double layer, yielding a local electric field $\mathbf{E}_{\text{coions}}$, the direction of which is opposite to that established by counterions, $\mathbf{E}_{\text{counterions}}$. Figure 1 illustrates the relative directions of these induced electric fields and the applied concentration gradient ∇n_0 for the case of a positively charged particle. Therefore, depending upon the operating conditions a particle may move toward the high- or low-concentration sides. Several attempts were made on the analyses of the diffusiophoresis of nonrigid particles,[18] particles covered by an ion-penetrable membrane layer,[19] charge-regulated particles, and a suspension of particles.[20−22]

* To whom correspondence should be addressed. Phone: 886-2-2363-7448. Fax: 886-2-23623040. E-mail: jphsu@ntu.edu.tw.

(1) Hunter, R. J. *Foundations of Colliod Science*; Clarendon Press: Oxford, 1989; Vol. *I*.
(2) Grushka, E.; Mccormick, R. M.; Kirkland, J. *J. Anal. Chem.* **1989**, *61*, 241.
(3) Knox, J. H.; Mccormick, R. M. *Chromatographia* **1994**, *38*, 207.
(4) Deryagin, B. V.; Dukhin, S. S.; Korotkova, A. A. *Kolloidn. Zh.* **1961**, *23*, 53.
(5) Deryagin, B. V.; Dukhin, S. S.; Korotkova, A. A. *Colloid J. USSR* **1978**, *40*, 531.
(6) Meisen, A; Bobkowic, A. J.; Cooke, N. E.; Farkas, E. J. *Can. J. Chem. Eng.* **1971**, *49*, 449.
(7) Prieve, D. C.; Gerhart, H. L.; Smith, R. E. *I&EC Product R&D* **1978**, *17*, 32.
(8) Smith, R. E.; Prieve, D. C. *Chem. Eng. Sci.* **1982**, *37*, 1213.
(9) Anderson, J. L.; Lowell, M. E.; Prieve, D. C. *J. Fluid Mech.* **1982**, *117*, 107.
(10) Keh, H. J.; Luo, S. C. *Phys. Fluids* **1995**, *7*, 2122.
(11) Keh, H. J.; Wan, Y. W. *Chem. Eng. Sci.* **2008**, *63*, 1612.
(12) Ebel, J. P.; Anderson, J. L.; Prieve, D. C. *Langmuir* **1988**, *4*, 397.
(13) Prieve, D. C. *CIT Eng. News* **1982**, *2*, 5.
(14) Dukhin, S. S.; Deryagin, B. V. *Surface and Colloid Science*; Wiley: New York, 1974; Vol. *7*.
(15) Prieve, D. C.; Anderson, J. L.; Ebel, J. P.; Lowell, M. E. *J. Fluid Mech.* **1984**, *148*, 247.
(16) Prieve, D. C.; Roman, R. *J. Chem. Soc., Faraday Trans. II* **1987**, *83*, 1287.
(17) Pawar, Y.; Solomentsev, Y. E.; Anderson, J. L. *J. Colloid Interface Sci.* **1993**, *155*, 488.
(18) Baygents, J. C.; Saville, D. A. *PCH Physicochem. Hydrodyn.* **1988**, *10*, 543.
(19) Misra, S.; Varanasi, S.; Varanasi, P. P. *Macromolecules* **1990**, *23*, 4258.
(20) Wei, Y. K.; Keh, H. J. *J. Colloid Interface Sci.* **2002**, *248*, 76.
(21) Hsu, J. P.; Lou, J.; He, Y. Y.; Lee, E. *J. Phys. Chem. B* **2007**, *111*, 2533.
(22) Keh, H. J.; Yu, L. L. *Langmuir* **2007**, *23*, 1061.

10.1021/la803334a CCC: $40.75
Published on Web 01/05/2009

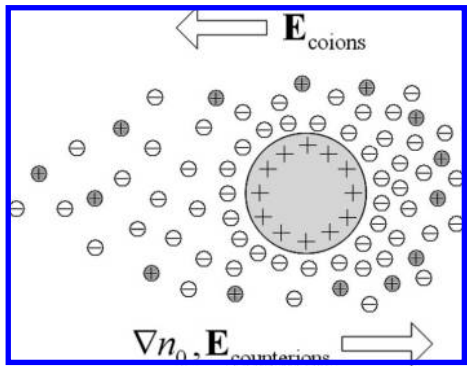

Figure 1. Two types of induced electric field in diffusiophoresis, $\mathbf{E}_{coions}$ and $\mathbf{E}_{counterions}$, arising, respectively, from two types of double-layer polarization for the case of a positively charged particle, where ∇n_0 is the applied concentration gradient.

In practice, diffusiophoresis needs be conducted in a finite space. That is, the diffusiophoretic behavior of a particle may be influenced by the presence of a boundary. Several attempts have been made recently on the boundary effect on diffusiophoresis. Lou and Lee,[23] for example, considered the diffusiophoresis of a sphere normal to a plane. The diffusiophoresis of a sphere between two parallel planes was analyzed by Chang and Keh[24] and Chen and Keh.[25] Note that the presence of a boundary can affect not only the hydrodynamic drag acting on the particle but also the degree of double-layer polarization, thereby making the problem complicated.

Similar to the possible presence of electroosmosis in the electrophoresis of a particle driven by an external electric field, diffusioosmosis, which includes chemiosmosis and electroosmosis, may be present in diffusiophoresis. Electroosmosis is caused by the induced electric field arising from double-layer polarization, and chemiosmosis arises from the nonuniform ionic distribution in the double layer surrounding a particle. In the latter, the higher concentration of counterions on the high-concentration side of the particle generates a diffusion flow along the particle surface toward its low-concentration side where the concentration of counterions is lower. Depending upon the boundary conditions assumed for the flow field on the particle−fluid interface, chemiosmosis may increase/decrease the hydrodynamic drag acting on the particle as it migrates toward the high/low-concentration side. Available results for diffusioosmosis are very limited in the literature.[26−28]

In this study, the boundary effect on the diffusiophoretic behavior of a particle is investigated by considering the diffusiophoresis of a sphere in a spherical cavity for arbitrary level of surface potential and thickness of double layer. The geometry chosen, although idealized, is capable of simulating the behavior of a particle in a porous media and approximating that in a cylindrical pore.[29] The influences of the thickness of the double layer, the level of surface potential, the size and position of the particle, the valence of ionic species, the electric Peclet number, and the charged conditions of the cavity on the diffusiophoretic velocity of the particle are discussed.

(23) Lou, J.; Lee, E. *J. Phys. Chem. C* **2008**, *112*, 2584.
(24) Chang, Y. C.; Keh, H. J. *J. Colloid Interface Sci.* **2008**, *322*, 634.
(25) Chen, P. Y.; Keh, H. J. *J. Colloid Interface Sci.* **2005**, *286*, 774.
(26) Keh, H. J.; Ma, H. C. *Langmuir* **2005**, *21*, 5461.
(27) Ma, H. C.; Keh, H. J. *J. Colloid Interface Sci.* **2006**, *289*, 476.
(28) Keh, H. J.; Ma, H. C. *Langmuir* **2007**, *23*, 2879.
(29) Zydney, A. L. *J. Colloid Interface Sci.* **1995**, *169*, 476.

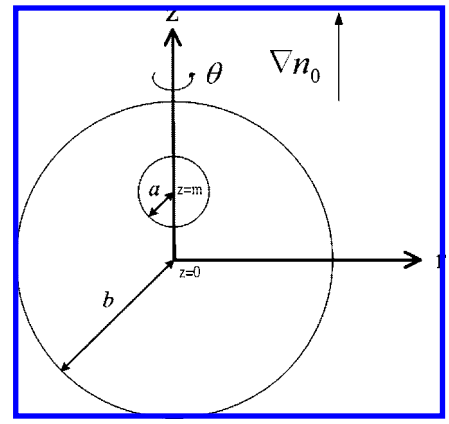

Figure 2. Diffusiophoresis of a spherical particle of radius a at an arbitrary position in a spherical cavity of radius b subject to an applied concentration gradient ∇n_0. The cylindrical coordinates (r, θ, z) are adopted with the origin at the center of the cavity; the direction of ∇n_0 is parallel to the z axis, and the center of the particle is at $z = m$.

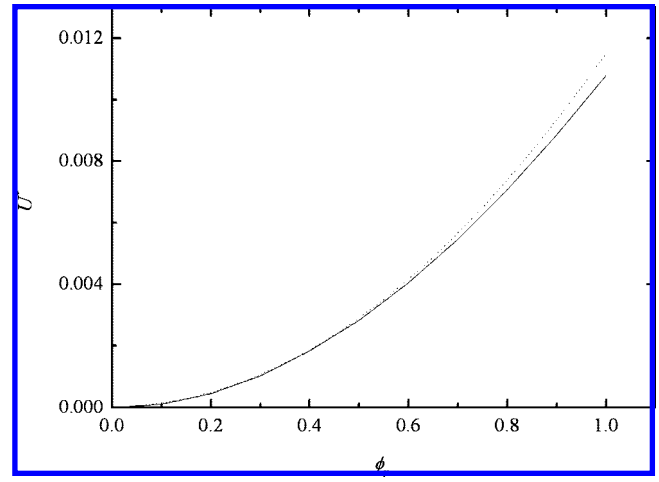

Figure 3. Variation of the scaled diffusiophoretic velocity U^* as a function of the scaled surface potential ϕ_r for a positively charged particle in an uncharged cavity at $P = 0\%$, $\lambda = 0.1$, $\kappa a = 1$, $\alpha = 1$, and $\beta = 0$. (Solid curve) Present numerical solution. (Dashed curve) Analytical solution for the case of an isolated sphere.[40]

Theory

Let us consider the diffusiophoresis of a nonconducting spherical particle of radius a at an arbitrary position in a spherical cavity of radius b illustrated in Figure 2. The cavity is filled with an aqueous, incompressible Newtonian fluid containing z_1:z_2 electrolytes, where z_1 and z_2 are the valence of cations and anions, respectively. Let $\lambda = a/b$ and $\alpha = -z_2/z_1$. The cylindrical coordinates (r, θ, z) are adopted with the origin located at the center of the cavity. The center of the particle is at $z = m$. A uniform concentration gradient ∇n_0 is applied in the z direction. Let ϕ and ζ_a be the electrical potential of the system and surface potential of the particle, respectively; ε, ρ, e, k_B, and T are the permittivity of the liquid phase, space charge density, elementary charge, Boltzmann constant, and absolute temperature, respectively; n_j, $\mathbf{J}_j$, and D_j are the number concentration, number flux, and diffusivity of ionic species j, respectively; $\mathbf{v}$, η, and p are the velocity, viscosity, and pressure of the liquid phase, respectively. Then the phenomenon under consideration can be described by

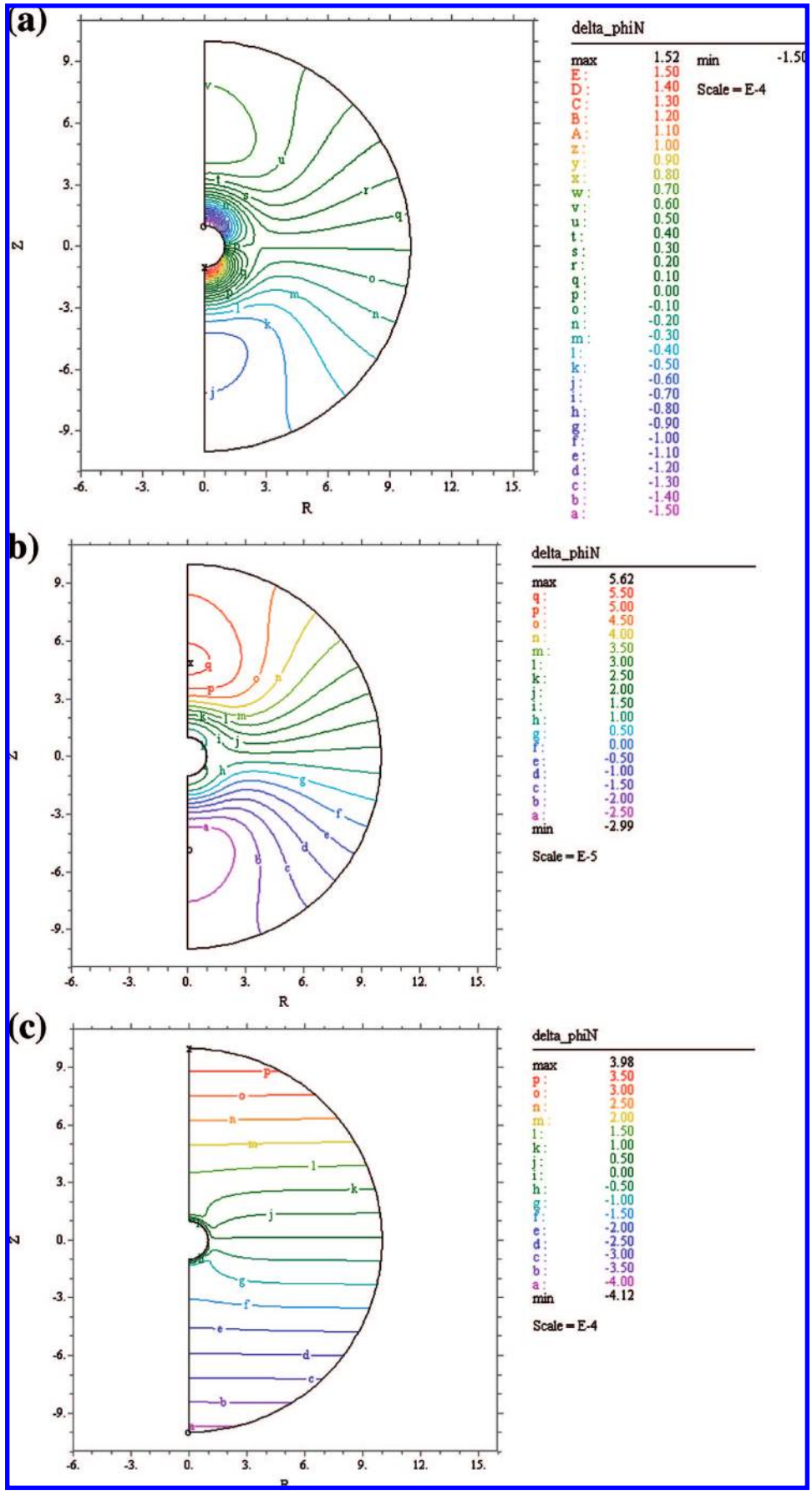

Figure 4. Contours of the scaled disturbed electric potential $\delta\phi^*$ (delta_phiN) at two levels of the scaled surface potential ϕ_r at $P = 0\%$, $\lambda = 0.1$, and $\alpha = 1$; $Z = z/a = z^*$, $R = r/a$. (a) $\phi_r = 1$, $\kappa a = 1$, and $\beta = 0$; (b) $\phi_r = 8$, $\kappa a = 1$, and $\beta = 0$; (c) $\phi_r = 5$, $\kappa a = 10$, and $\beta = -0.2$.

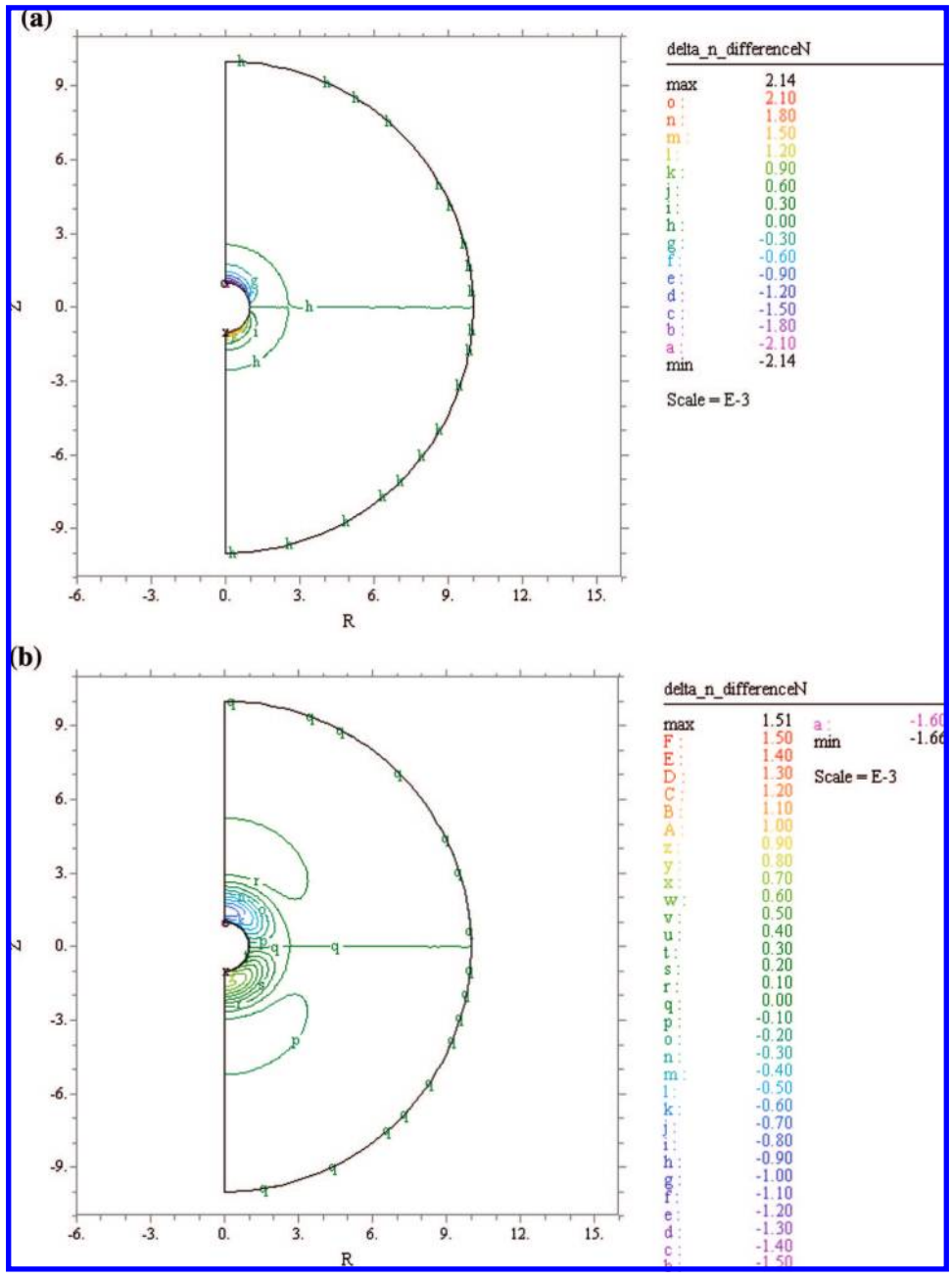

Figure 5. Contours of the scaled net concentration difference *CD* (delta_n_differenceN){=[$(n_1 - n_{10}) - (n_2 - n_{20})$]/$n_{e0}$} at two levels of the scaled surface potential ϕ_r at $P = 0\%$, $\lambda = 0.1$, $\kappa a = 1$, $\alpha = 1$, and $\beta = 0$; $Z = z/a = z^*$, $R = r/a$: (a) $\phi_r = 1$, (b) $\phi_r = 8$.

$$\nabla^2\phi = -\frac{\rho}{\varepsilon} = -\sum_{j=1}^{2}\frac{z_j e n_j}{\varepsilon} \quad (1)$$

$$\nabla \cdot \mathbf{J}_j = 0 \quad (2)$$

$$\mathbf{J}_j = -D_j\left(\nabla n_j + \frac{z_j e}{k_B T} n_j \nabla\phi\right) + n_j \mathbf{v} \quad (3)$$

$$\nabla \cdot \mathbf{v} = 0 \quad (4)$$

$$-\nabla p + \eta\nabla^2 v - \rho\nabla\phi = 0 \quad (5)$$

where ∇^2 is the Laplace operator.

Similar to the treatment of O'Brien and White[30] in the analysis of the electrophoresis driven by an applied electric field, we let $\phi = \phi_e + \delta\phi$, where ϕ_e and $\delta\phi$ are the equilibrium potential (the potential in the absence of ∇n_0) and a perturbed potential arising from application of ∇n_0, respectively. In addition, let

$$n_j = n_{j0e}\exp\left[-\frac{z_j e(\phi_e + \delta\phi + g_j)}{k_B T}\right] \quad (6)$$

where g_j is a perturbed function simulating the deformation of the double layer due to the convection flow and n_{j0e} is the bulk ionic concentration at equilibrium.

Suppose that $a|\nabla n_0| \ll n_{0e}$, where n_{0e} is the bulk solute concentration at equilibrium. That is, after application of ∇n_0, the concentration of solute is only slightly nonuniform over the length scale a. In this case, it can be shown that eqs 1, 2, and 6 yield[21,31,32]

(30) O'Brien, R. W.; White, L. R. *J. Chem. Soc., Faraday Trans. 2* **1978**, *74*, 1607.

(31) Lee, E; Chu, J. W.; Hsu, J. P. *J. Colloid Interface Sci.* **1997**, *196*, 316.
(32) Hsu, J. P.; Chen, Z. C. *J. Colloid Interface Sci.* **2007**, *314*, 256.

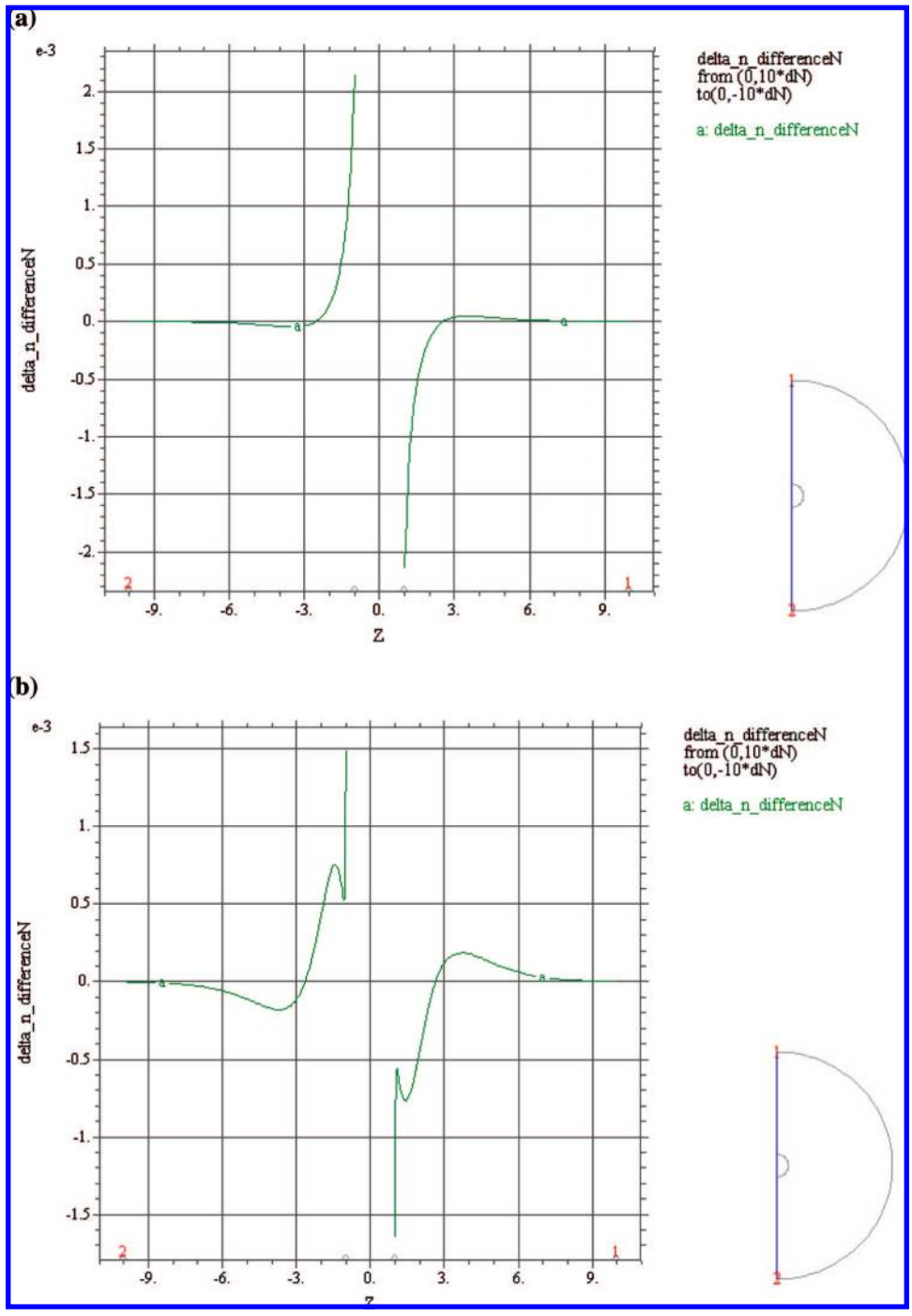

Figure 6. Spatial variation in the scaled net concentration difference *CD* (delta_n_differenceN) {=[$(n_1 - n_{10}) - (n_2 - n_{20})$]/$n_{e0}$} at two levels of the scaled surface potential ϕ_r for the case of Figure 5.

$$\nabla^{*2}\phi_e^* = -\frac{(\kappa a)^2}{\phi_r(1+\alpha)}[\exp(-\phi_r\phi_e^*) - \exp(\alpha\phi_r\phi_e^*)] \quad (7)$$

$$\nabla^{*2}\delta\phi^* - \frac{(\kappa a)^2}{1+\alpha}[\exp(-\phi_r\phi_e^*) + \alpha\exp(\alpha\phi_r\phi_e^*)]\delta\phi^* = \frac{(\kappa a)^2}{1+\alpha}[\exp(-\phi_r\phi_e^*)g_1^* + \exp(\alpha\phi_r\phi_e^*)\alpha g_2^*] \quad (8)$$

$$\nabla^{*2}g_1^* - \phi_r\nabla^*\phi_e^*\cdot\nabla^* g_1^* = \gamma \mathrm{Pe}_1 \mathbf{v}^*\cdot\nabla^*\phi_e^* \quad (9)$$

$$\nabla^{*2}g_2^* + \alpha\phi_r\nabla^*\phi_e^*\cdot\nabla^* g_2^* = \gamma \mathrm{Pe}_2 \mathbf{v}^*\cdot\nabla^*\phi_e^* \quad (10)$$

$$n_1^* = \exp(-\phi_r\phi_e^*)[1 - \phi_r(\delta\phi^* + g_1^*)] \quad (11)$$

$$n_2^* = \exp(\alpha\phi_r\phi_e^*)[1 + \phi_r(\delta\phi^* + g_2^*)] \quad (12)$$

Here, $\nabla^* = a\nabla$ and $\nabla^{*2} = a^2\nabla^2$ are the scaled gradient operator and the scaled Laplace operator, respectively; $\phi_r = \zeta_a z_1 e/k_B T$ is the scaled surface potential. $\kappa = [\sum_{j=1}^{2} {}_{j0e}(ez_j)^2 / \varepsilon\, k_B T]^{1/2}$ is the reciprocal Debye length, $n_j^* = n_j/n_{j0e}$, $\phi_j^* = \phi_j/\zeta_a$, $g_j^* = g_j/\zeta_a$, and $\mathrm{Pe}_j = \varepsilon(k_B T/z_1 e)^2/\eta D_j$ is the electric Peclet number, $j = 1, 2$. $\mathbf{v}^* = \mathbf{v}/U^0$, where $U^0 = \varepsilon\gamma\,(k_B T/z_1 e)^2/a\eta$ is a reference velocity, $\gamma = \nabla^* n_0^*$ is the scaled concentration gradient imposed to the system, and $n_0^* = n_0/n_{0e}$.

In terms of the scaled symbols, the flow field can be described by[31−33]

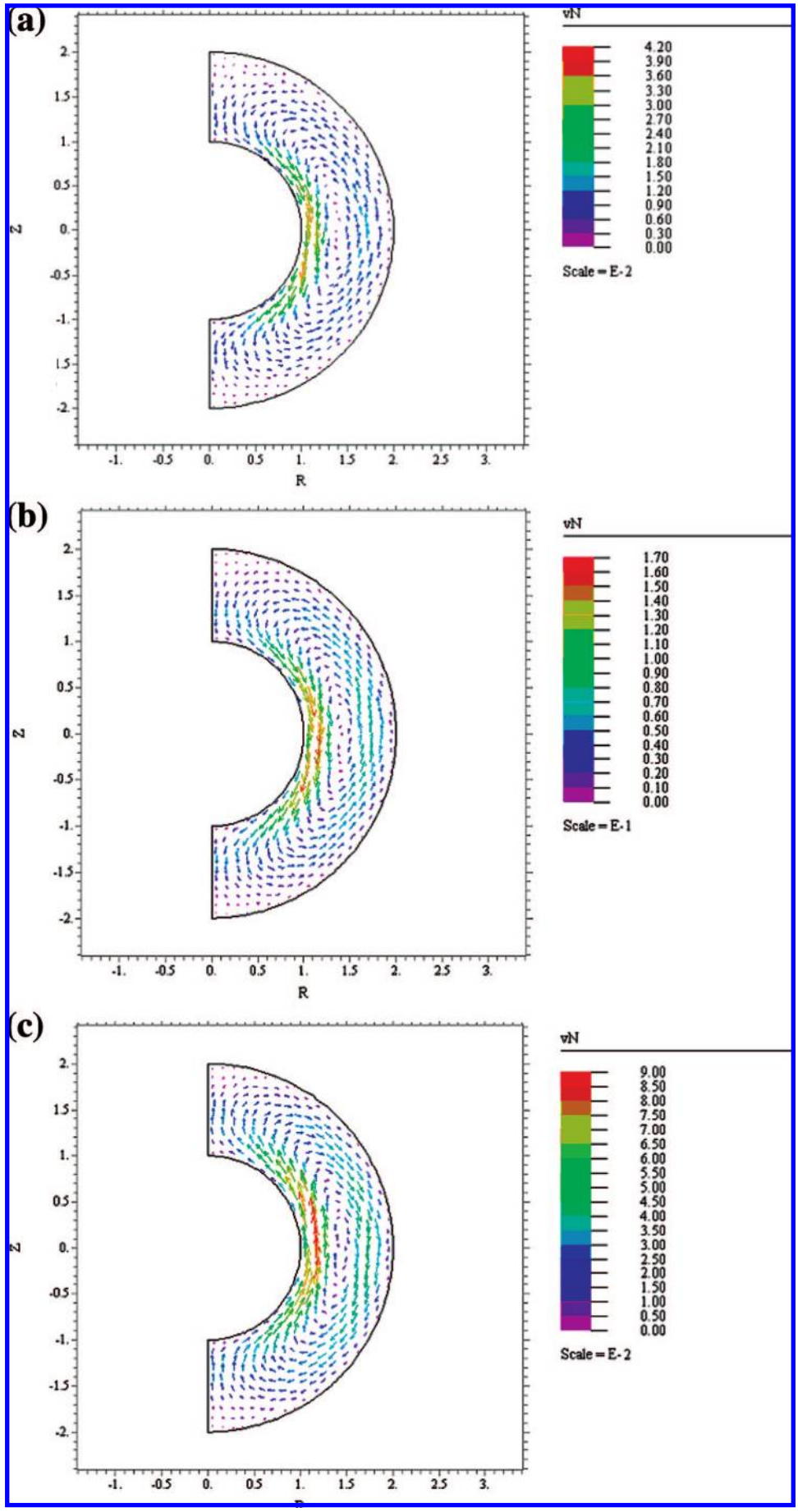

Figure 7. Contours of the scaled velocity in the second subproblem for various combinations of ϕ_r and β at $P = 0\%$, $\lambda = 0.5$, $\kappa a = 5$, and $\alpha = 1$: (a) $\phi_r = 1$ and $\beta = 0$; (b) $\phi_r = 1$ and $\beta = 0.64$; (c) $\phi_r = -1$ and $\beta = 0.64$.

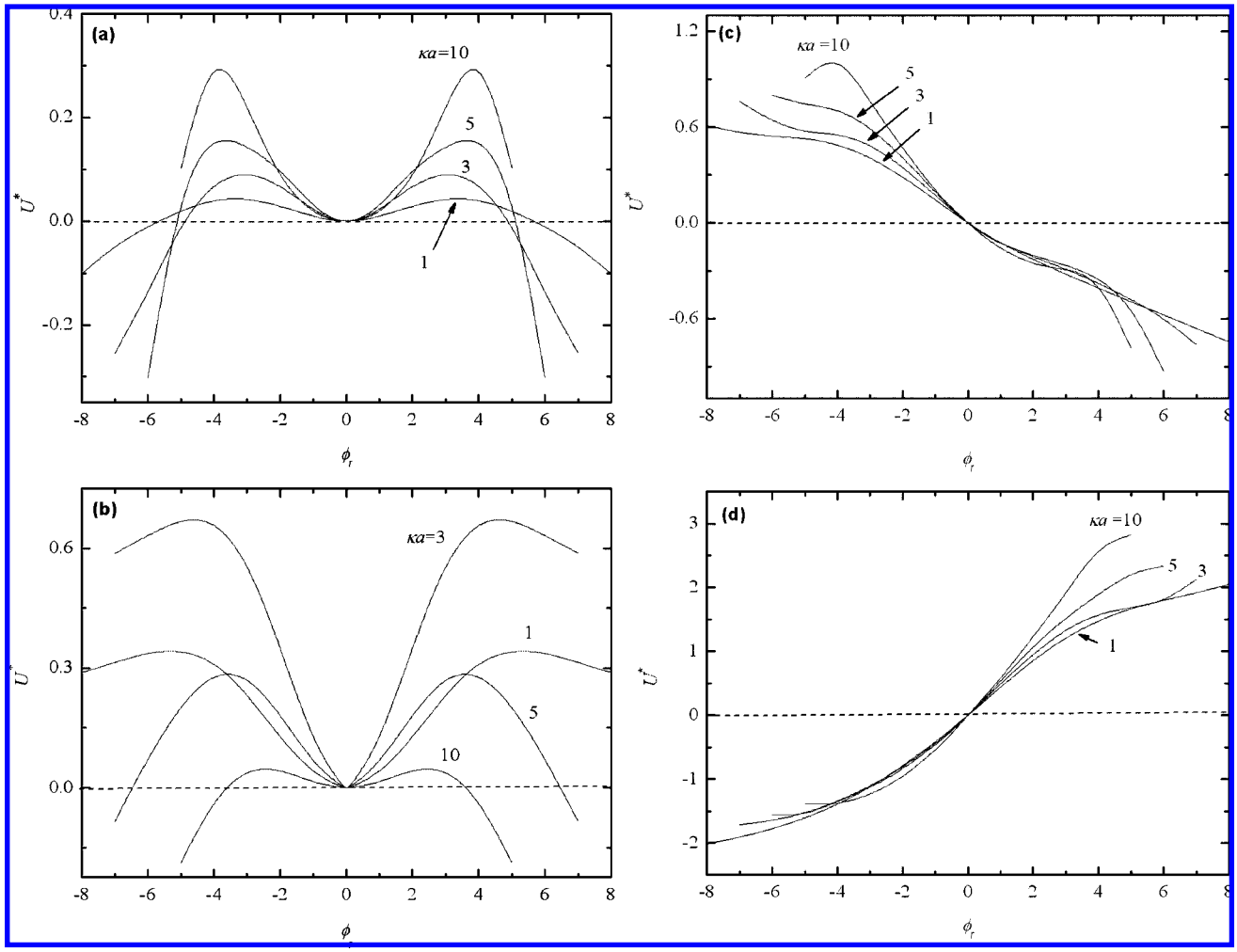

Figure 8. Variations of the scaled diffusiophoretic velocity U^* as a function of the scaled surface potential ϕ_r at various combinations of κa, β, and λ at $P = 0\%$ and $\alpha = 1$: (a) $\lambda = 0.1$ and $\beta = 0$; (b) $\lambda = 0.5$ and $\beta = 0$; (c) $\lambda = 0.1$ and $\beta = -0.2$; (d) $\lambda = 0.1$ and $\beta = 0.64$.

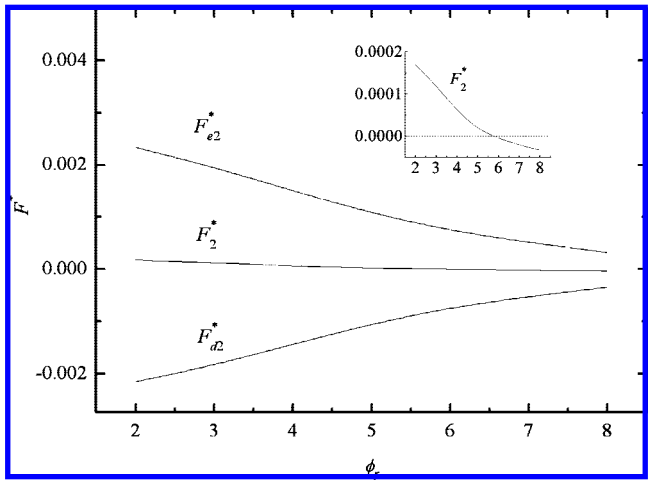

Figure 9. Variations of the scaled forces F^*_{e2}, F^*_{d2}, and F^*_2, where $F^*_2 = F_2/\varepsilon\zeta_a^2 a^2$, as a function of the scaled surface potential ϕ_r at $P = 0\%$, $\lambda = 0.1$, $\kappa a = 1$, $\alpha = 1$, and $\beta = 0$.

$$\nabla^* \cdot \mathbf{v}^* = 0 \tag{13}$$

$$-\varphi_r^2 \nabla^* p^* + \gamma \nabla^{*2} \mathbf{v}^* + \varphi_r^2 \nabla^{*2} \varphi^* \nabla^* \varphi^* = 0 \tag{14}$$

where $p^* = p/p_{ref}$ with $p_{ref} = \varepsilon\zeta_a^2/a^2$.

The following boundary conditions are assumed for eqs 7−10, 13, and 14

$$\phi_e^* = 1 \text{ on the particle surface} \tag{15}$$

$$\phi_e^* = 0 \text{ on the cavity surface} \tag{16}$$

$$\mathbf{n} \cdot \nabla^* \delta\phi^* = 0 \text{ on the particle surface} \tag{17}$$

$$\mathbf{n} \cdot \nabla^* \delta\phi^* = \frac{1}{\phi_r R^*} \beta\gamma z^* \text{ on the cavity surface} \tag{18}$$

$$\mathbf{n} \cdot \nabla^* g_j^* = 0 \text{ on the particle surface} \tag{19}$$

$$g_1^* = -\frac{1}{\phi_r} z^* \gamma - \delta\phi^* \text{ on the cavity surface} \tag{20}$$

$$g_2^* = \frac{1}{\alpha\phi_r} z^* \gamma - \delta\phi^* \text{ on the cavity surface} \tag{21}$$

$$\mathbf{v}^* = U^* \mathbf{e}_z \text{ on the particle surface} \tag{22}$$

$$\mathbf{v}^* = 0 \text{ on the cavity surface} \tag{23}$$

In these expressions, $\beta = [D_1 - D_2]/[D_1 + \alpha D_2]$ and $U^* = U/U^0$, where U is the speed of the sphere. $z^* = z/a$, $R^* = R/a$, $\mathbf{n}$ is the unit normal vector directed into the liquid phase, and $\mathbf{e}_z$ is the unit vector in the z direction. Here, we assume that both the surface of the particle and that of the cavity are nonconductive, nonslip, and impermeable to ionic species and the concentration of ionic species reaches the corresponding bulk value on the cavity surface. Equation 18 arises from the assumption that the

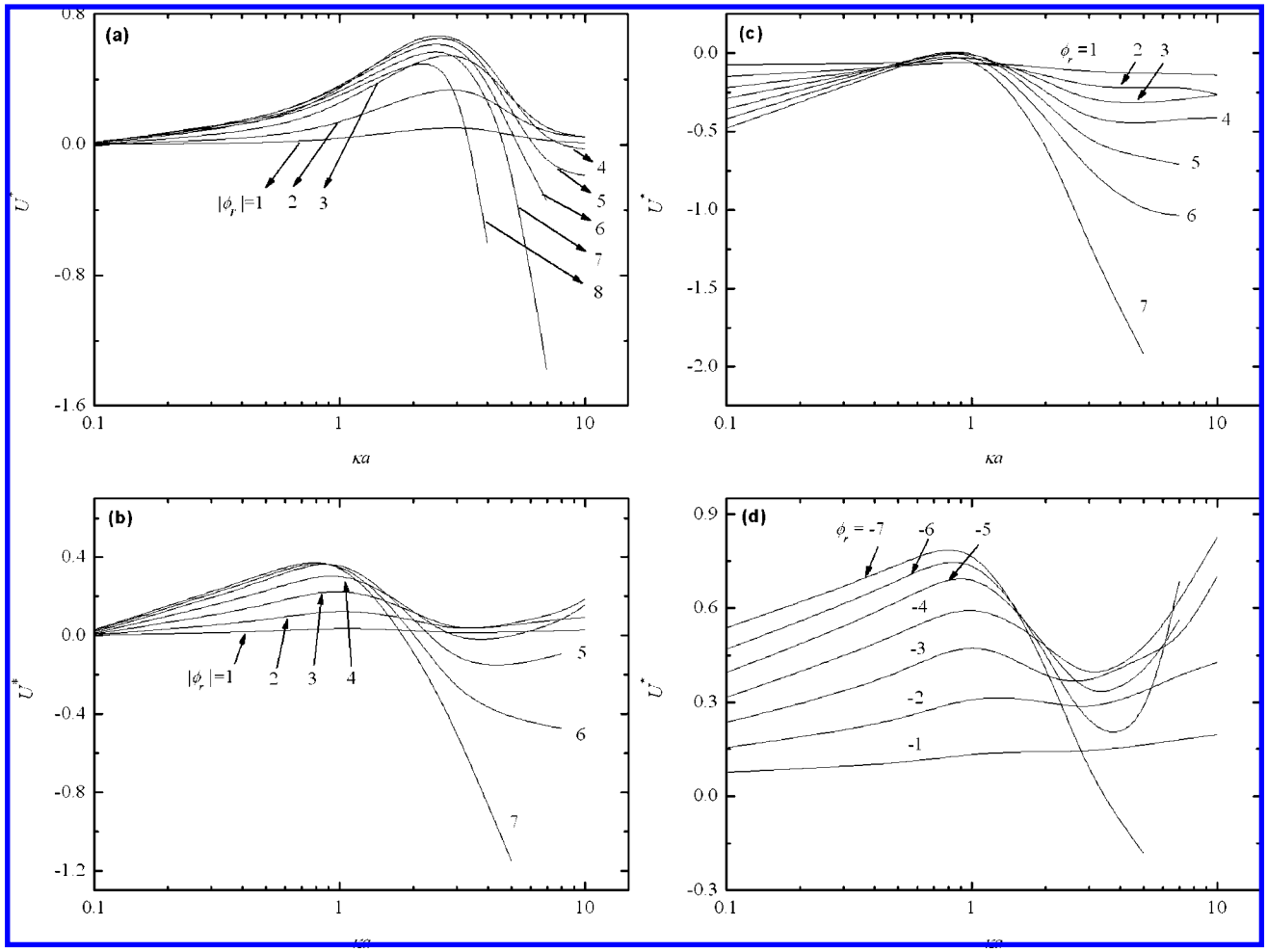

Figure 10. Variations of the scaled diffusiophoretic velocity U^* as a function of κa at various combinations of ϕ_r, β, and λ at $P = 0\%$ and $\alpha = 1$: (a) $\lambda = 0.5$ and $\beta = 0$; (b) $\lambda = 0.3$ and $\beta = 0$; (c) $\phi_r < 0$, $\lambda = 0.3$, and $\beta = -0.2$; (d) $\phi_r < 0$, $\lambda = 0.3$, and $\beta = -0.2$.

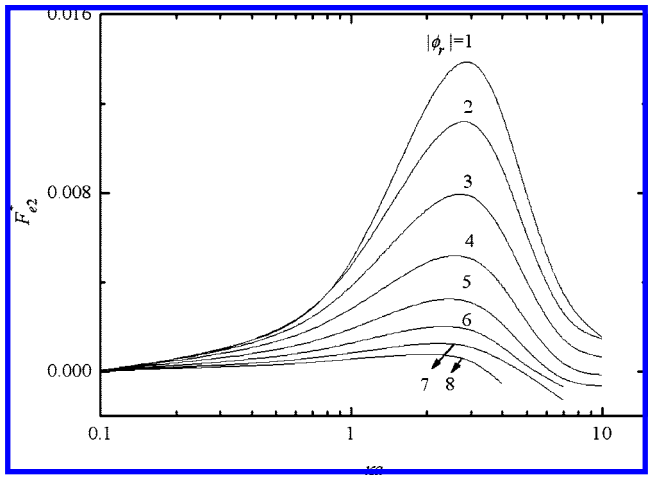

Figure 11. Variation of the scaled electrical force F^*_{e2} as a function of κa for the case of Figure 10a.

net charge flux ($z_1\mathbf{J}_1 + z_2\mathbf{J}_2$) vanishes on the cavity surface.[20,24] Equation 19 implies that the surface of the particle is ion impenetrable,[34] and eqs 20 and 21 assume that the ionic concentrations on the cavity surface reach the value $n_{j0e} + z\nabla n_{j0}$.[21,23,35] Note that if $\beta > 0$ the background electric field arising from the difference in the ionic mobilities has the same direction as that of the imposed concentration gradient. On the other hand, if $\beta < 0$ they have opposite directions, and if $\beta = 0$ the background electric field vanishes.

Adopting the treatment of O'Brien and White in the analysis of the electrophoresis of a charged particle driven by an applied electrical field[30] the present problem is partitioned into two subproblems. In the first subproblem the particle moves at a constant velocity U in the absence of ∇n_0. In the second subproblem ∇n_0 is applied but the particle is remains fixed in the space. If we let $\mathbf{F_i}$ be the total force acting on the particle in the z direction in subproblem i, and F_i be its magnitude, then $F_1 = \chi_1 U$ and $F_2 = \chi_2 \nabla n_0$. Note that χ_1 is independent of U, and χ_2 is independent of ∇n_0. Assuming steady-state condition, then $F_1 + F_2 = 0$, which yields

$$U = -\frac{\chi_2}{\chi_1}\nabla n_0 \tag{24}$$

In our case, the forces acting on the particle include the electrical force $\mathbf{F_e}$ and the hydrodynamic force $\mathbf{F_d}$. Let F_{ei} and F_{di} be the z components of $\mathbf{F_e}$ and $\mathbf{F_d}$ in subproblem i, respectively, and $F^*_{ei} = F_{ei}/\varepsilon\zeta_a^2 a^2$ and $F^*_{di} = F_{di}/\varepsilon\zeta_a^2 a^2$ are the corresponding scaled

(33) Masliyah, J. H.; Bhattacharjee, S. *Electrokinetic transport phenomena*, 4th ed.; Wiley: New York, 2006.
(34) Lee, E.; Chu, J. W.; Hsu, J. P. *J. Chem. Phys.* **1999**, *110*, 11643.
(35) Lou, J.; He, Y. Y.; Lee, E. *J. Colloid Interface Sci.* **2006**, *299*, 443.

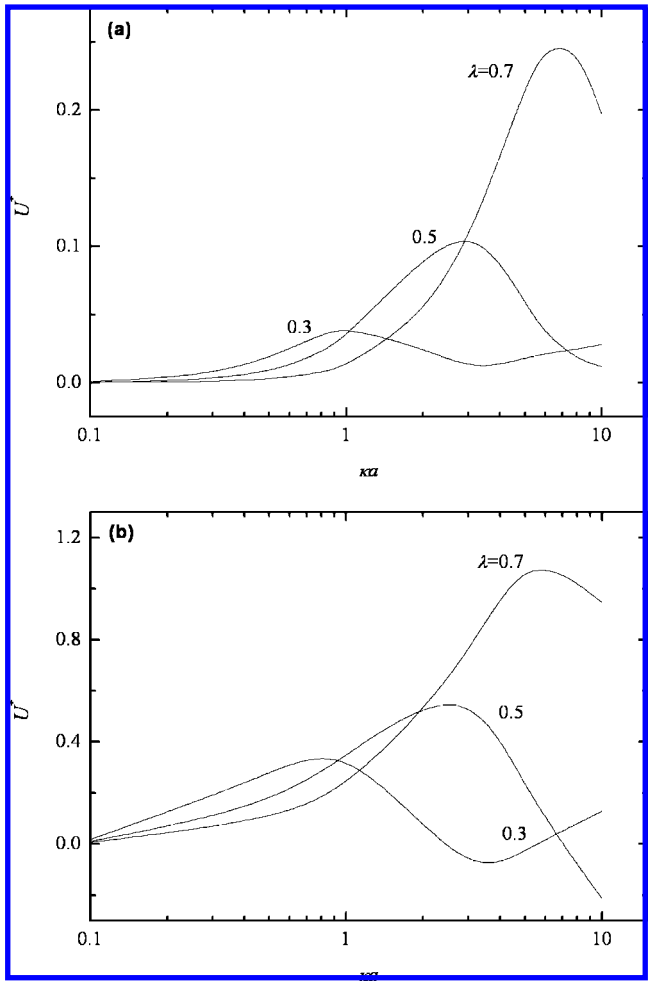

Figure 12. Variations of the scaled diffusiophoretic velocity U^* as a function of κa at various combinations of λ and ϕ_r at $P = 0\%$, $\alpha = 1$, and $\beta = 0$: (a) $|\phi_r| = 1$, (b) $|\phi_r| = 5$.

quantities. It can be shown that F_{ei}[36,37] and F_{di}[38] can be evaluated, respectively, by

$$F_{ei}^* = \int_{S^*} \left(\frac{\partial \phi_e^*}{\partial n} \frac{\partial \delta \phi^*}{\partial \hat{z}} - \frac{\partial \phi_e^*}{\partial t} \frac{\partial \delta \phi^*}{\partial t} \right) dS^* \qquad (25)$$

and

$$F_{di}^* = \int_{S^*} (\sigma^{H^*} \cdot \mathbf{n}) \cdot \mathbf{e}_z \, dS^* \qquad (26)$$

Here, $S^* = S/a^2$ is the scaled surface area, S being the particle surface; n and t are the magnitude of the unit normal vector and that of the unit tangential vector, respectively, and $\hat{z}$ is the z component of the unit normal vector. $\sigma^{H^*} = \sigma^H/\varepsilon\zeta_a^2$ is the scaled shear stress tensor, σ^H being the shear stress tensor.

Results and Discussion

The governing equations and associated boundary conditions are solved numerically by FlexPDE.[39] The applicability of this software is justified by using it to solve the diffusiophoresis of an isolated, positively charged sphere in an infinite aqueous KCl solution where an analytical solution is available. In this case, $\beta = 0$ and $Pe_1 = Pe_2 = 0.26$.[20,21,35,40,41] Figure 3 shows the variation of the scaled diffusiophoretic velocity $U^* = U/U^0$ as a function of the scaled surface potential ϕ_r. Both the approximate analytical result,[40] which is valid only for low values of ϕ_r, and the present numerical result are presented. As seen in Figure 3, the performance of the software adopted is satisfactory. As expected, the larger the value of ϕ_r the larger the deviation of the approximate analytical result from the exact numerical result.

The diffusiophoretic behaviors of a particle under various conditions are examined through numerical simulation. For illustration, we assume that the particle is charged (positively or negatively) and the cavity is uncharged. Three values are assumed for β: 0.0, −0.2, and 0.64.[21] These correspond to the cases where the electrolytes in the liquid phase are KCl ($Pe_1 = Pe_2 = 0.26$), NaCl ($Pe_1 = 0.39$, $Pe_2 = 0.26$), and HCl ($Pe_1 = 0.057$, $Pe_2 = 0.26$).[20,21,35,40,41]

In our case, the ionic concentration near the top region of the particle is higher than that near its bottom region, and therefore, the thickness of the double layer near the top of the particle is thinner than that near its bottom. If the particle is positively charged, the amount of anions (counterions) inside the double layer on the high-concentration side is greater than that on the low-concentration side. This kind of double-layer polarization, defined as type I double-layer polarization, for convenience, yields an induced electric field, which drives the particle upward. In Figure 4 the particle is positively charged, and according to Figure 4a, the scald perturbed potential $\delta\phi^*$ is negative on the high-concentration side (region near the top of the particle), implying that the rate of decline in the potential is faster than that if ∇n_0 is not applied. This arises because the double layer near the top of the particle is thinner than that if ∇n_0 is not applied. On the other hand, $\delta\phi^*$ is positive on the low-concentration side (region near the bottom of the particle), implying that the rate of decline in the potential is slower than that if ∇n_0 is not applied. Figure 4b suggests that if ϕ_r is sufficiently high another kind of double-layer polarization, defined as type II double-layer polarization in subsequent discussion, is present. Because the cations come from the applied ∇n_0 accumulating near the outer boundary of the double layer on the high-concentration side, the concentration of cations (coions) over there is higher than that on the low-concentration side. This yields an induced electric field, the direction of which is opposite to that arises from type I double-layer polarization, and generates an electric force pushing the particle toward the low-concentration side. Figure 4c shows that if $\beta \neq 0$ (i.e., $D_1 \neq D_2$) an induced electric field is established, as predicted by eq 18. In this case, an electric field arising from the electrostatic interaction between ions is present to make the net ionic flux vanish. Otherwise, charges will accumulate in some region in the bulk phase, which violates electroneutrality. As seen in Figure 4 the $\delta\phi^*$ contributed by the effect of double-layer polarization is appreciable. Note that if the strength of the induced electric field arising from type II double-layer polarization exceeds that arising from type I double-layer polarization, then the net electric force drives the particle toward the low-concentration side. We define the scaled net ionic concentration difference, CD, as $CD = \{[(n_1 - n_{1e}) - (n_2 - n_{2e})]/n_{e0}\}$, which measures the increase in the net charge arising from application of ∇n_0. As seen in Figures 5 and 6 if the particle is positively charged CD is negative in the region near two times the particle radius from the particle surface on the high-concentration side and positive on the low-concentration side, implying that the increased number of anions (counterions)

(36) Hsu, J. P.; Yeh, L. H.; Ku, M. H. *J. Colloid Interface Sci.* **2007**, *305*, 324.
(37) Hsu, J. P.; Yeh, L. H. *J. Chin. Inst. Chem. Eng.* **2006**, *37*, 601.
(38) Happel, J.; Brenner, H. *Low-Reynolds Number Hydrodynamics*; Nijhoff: Boston, 1983.
(39) *FlexPDE*, version 2.22; PDE Solutions Inc.: Spokane Valley, WA, 2001.
(40) Keh, H. J.; Wei, Y. K. *Langmuir* **2000**, *16*, 5289.
(41) Chun, B.; Ladd, A. J. C. *J. Colloid Interface Sci.* **2004**, *274*, 687.

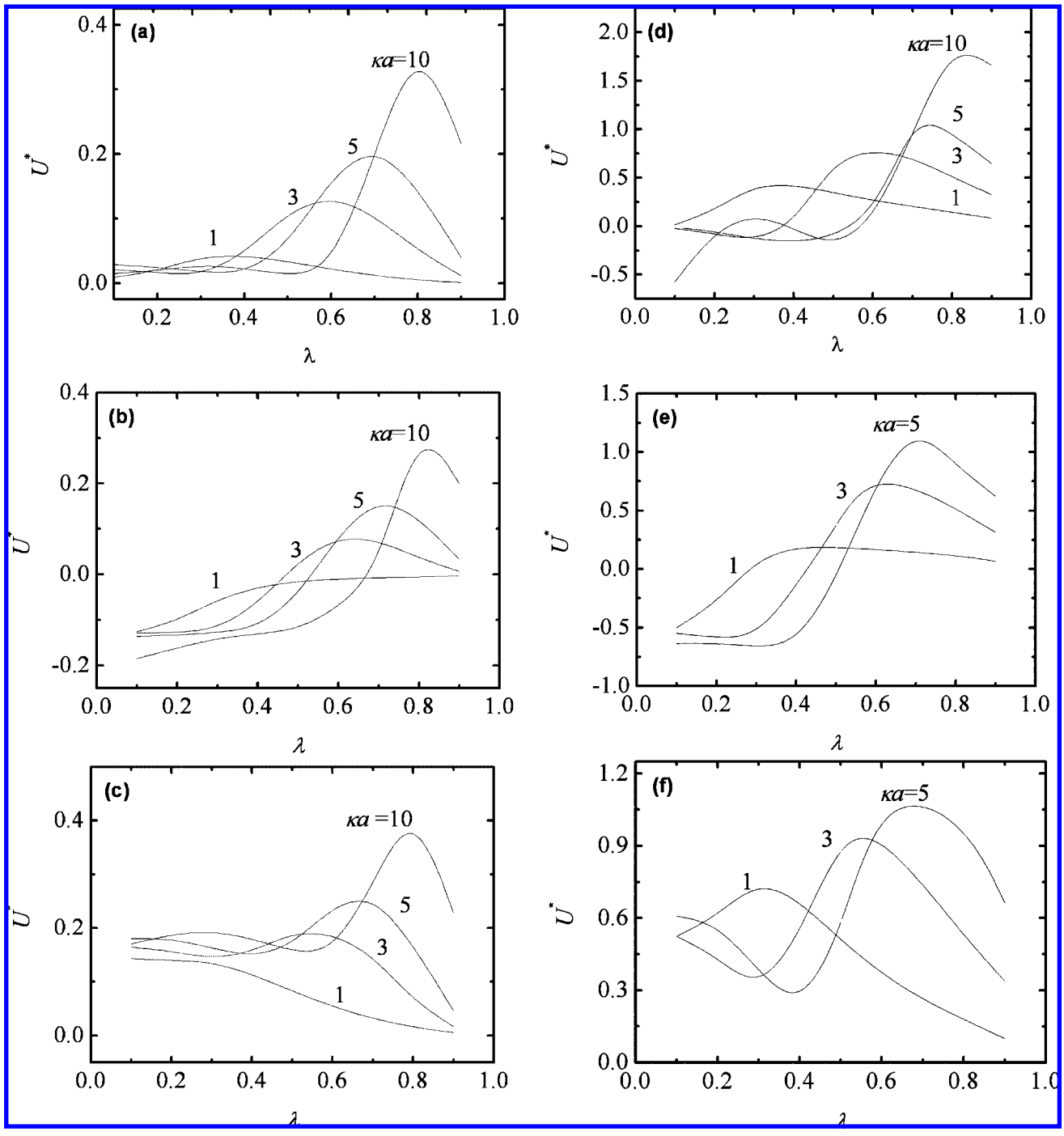

Figure 13. Variations of the scaled diffusiophoretic velocity U^* as a function of λ at various combinations of ϕ_r and β at $P = 0\%$ and $\alpha = 1$: (a) $|\phi_r| = 1$ and $\beta = 0$; (b) $\phi_r = 1$ and $\beta = -0.2$; (c) $\phi_r = -1$ and $\beta = -0.2$; (d) $|\phi_r| = 5$ and $\beta = 0$; (e) $\phi_r = 5$ and $\beta = -0.2$; (f) $\phi_r = -5$ and $\beta = -0.2$.

is greater than that of cations on the high-concentration side but less on the low-concentration side. That is, application of ∇n_0 leads to type I double-layer polarization and the particle is driven toward the high-concentration side. If ϕ_r is sufficiently high (=8), *CD* is positive in the region approximately 2.5−8 times the particle radius from the particle surface on the high-concentration side. That is, the increase in the amount of cations (coions) near the outer region of the high-concentration side of the double layer due to application of ∇n_0 is greater than that of anions. This arises from the strong electrostatic repulsive force between the particle and the cations in the double layer, and only anions can be present with an appreciable amount in the double layer. As a result, type II double-layer polarization occurs, the direction of the corresponding induced electric field is opposite to that of ∇n_0, and the particle is driven toward the low-concentration side (upward).

The unbalanced amount of counterions in the double layer on the high- and low-concentration sides of a particle arising from application ∇n_0 leads to a diffusion flow. This is illustrated in Figure 7, which shows the flow field in the second subproblem, where ∇n_0 is applied but the particle is remains fixed. As seen in Figure 7a the fluid near the positively charged particle flows from the high-concentration side to the low-concentration side along the surface of the particle. Because $\beta = 0$ in the present case, it is a chemiosmotic flow. Note that the corresponding fluid flow along the cavity surface is from the low-concentration side

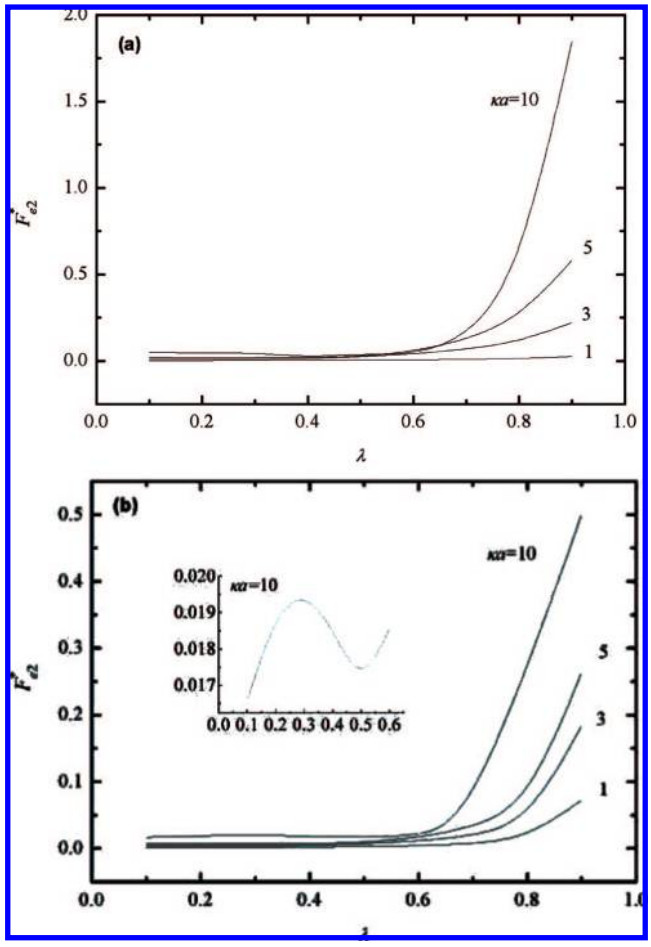

Figure 14. Variations of the scaled electrical force F^*_{e2} as a function of λ at various values of κa at $P = 0\%$, $\alpha = 1$, and $\beta = 0$: (a) $|\phi_r| = 1$, (b) $|\phi_r| = 5$.

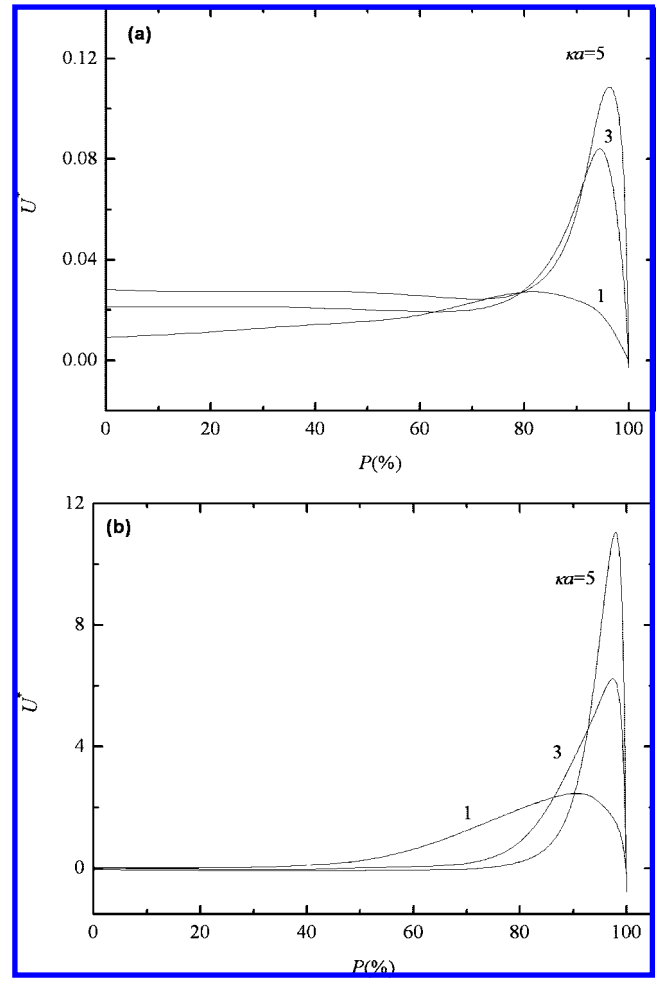

Figure 15. Variations of the scaled diffusiophoretic velocity U^* as a function of the position parameter P at various combinations of κa and ϕ_r for a charged particle in an uncharged cavity at $\lambda = 0.1$, $\alpha = 1$, and $\beta = 0$: (a) $|\phi_r| = 1$, (b) $|\phi_r| = 5$.

to the high-concentration side. In Figure 7b the particle is positively charged and $\beta > 0$. In this case, in addition to the chemiosmotic flow, an electroosmotic flow is also present. Because the direction of this electroosmotic flow is the same as that of ∇n_0, the velocity of the diffusioosmotic flow is faster than that in Figure 7a. In the case of Figure 7c the particle is negatively charged and $\beta > 0$; the chemiosmotic flow and the corresponding electroosmotic flow have the opposite directions. Because under the conditions assumed the electroosmotic flow is stronger than the corresponding chemiosmotic flow, the combined fluid flow is in the opposite direction as that in Figures 7a and 7b.

Figure 8 shows the variations of the scaled diffusiophoretic velocity $U^* = U/U^0$ as a function of the scaled surface potential ϕ_r at various combinations of κa, β, and λ. As seen in Figure 8a because $\beta = 0$, U^* is symmetric about $\phi_r = 0$. If λ is small (=0.1), that is, the boundary effect is relatively unimportant, U^* has a local maximum as $|\phi_r|$ varies and the larger the κa the larger the local maximum. The presence of the local maximum arises from the competition of the electric forces due to types I and II double-layer polarization and the drag due to chemiphoretic flow. As illustrated in Figures 4b, 5b, and 6b the effect of type II double-layer polarization increases with increasing $|\phi_r|$, leading to a decrease in U^*. If $|\phi_r|$ is sufficiently high, the sum of the effect of osmotic flow (chemiphoretic in Figures 8a and 8b and diffusiophoretic in Figures 8c and 8d) and that of type II double-layer polarization is more significant than that of type I double-layer polarization and U^* becomes negative. On the other hand, if $|\phi_r|$ is low, the effect of type II double-layer polarization is relatively more unimportant than that of type I double-layer polarization and U^* is positive. As seen in Figure 9, F^*_{e2} declines with increasing ϕ_r, because type II double-layer polarization is significant at high ϕ_r. However, F^*_{e2} remains positive at $\phi_r = 8$, implying that the electric force arising from type I double-layer polarization is still greater than that arising from type II double-layer polarization. Therefore, the observed negative value of U^* is not because F^*_{e2} is negative; it is because the reduction of F^*_{e2} makes $(F^*_{e2} + F^*_{d2})$ negative. It is interesting to see that if λ is sufficiently large (>0.5), the local maximum of U^* exhibits a maximum as κa varies. Note that if ϕ_r is sufficiently high, U^* becomes negative, that is, the particle moves in the $-z$ direction. The presence of the local maximum arises mainly from the competition between the effects of type I and type II double-layer polarization due to application of ∇n_0. Figure 8c reveals that if $\beta < 0$ the direction of the induced electric field arising from $D_1 \neq D_2$ is opposite to that of ∇n_0 and drives a positive/negative-charged particle toward the low/high-concentration region. On the other hand, if $\beta > 0$ the induced electric field has the same direction as that of ∇n_0 and drives a positive/negative-charged particle toward the high/low-concentration region, as seen in Figure 8d. We conclude that if $|\beta|$ is large, migration of a particle is dominated by electrophoresis and if $|\beta|$ is small by chemiphoresis.

The variation in the scaled diffusiophoretic velocity U^* as a function of κa for the case where the boundary effect becomes

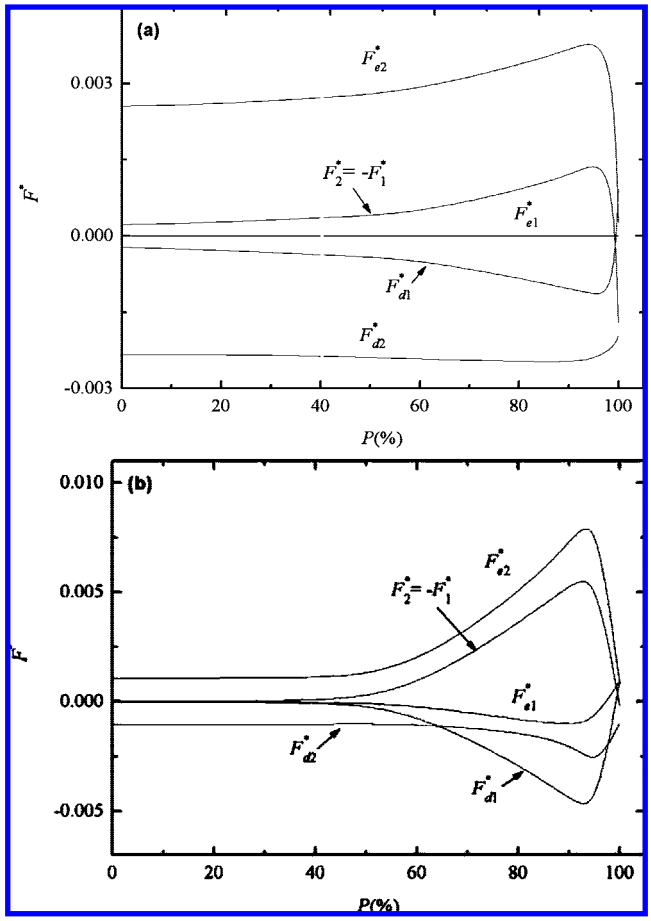

Figure 16. Variations of the scaled forces F^*_{e1}, F^*_{e2}, F^*_{d1}, F^*_{d2}, $-F^*_1$, and F^*_2, where $F^*_j = F_j/\varepsilon\zeta_d^2 a^2$, $j = 1$ and 2, as a function of the position parameter P at $\lambda = 0.1$, $\kappa a = 1$, $\alpha = 1$, and $\beta = 0$: (a) $|\phi_r| = 1$, (b) $|\phi_r| = 5$.

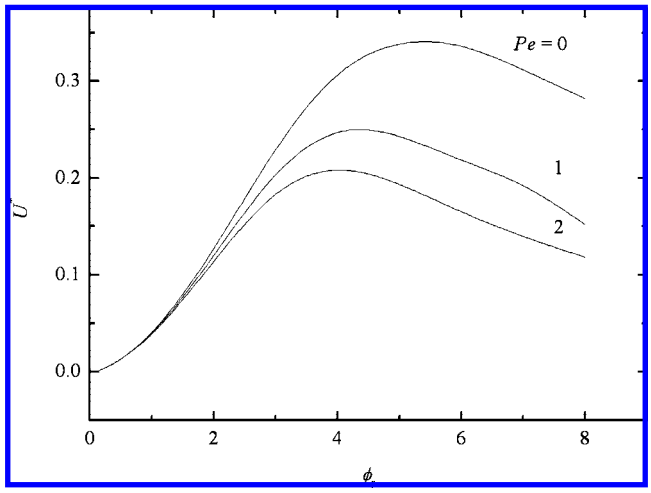

Figure 17. Variations of the scaled diffusiophoretic velocity U^* as a function of the scaled surface potential ϕ_r at various values of Pe (=Pe_1 = Pe_2) at $P = 0\%$, $\lambda = 0.5$, $\kappa a = 1$, $\alpha = 1$, and $\beta = 0$.

appreciable is presented in Figure 10. This figure indicates that the influence of the cavity on the diffusiophoretic behavior of the particle is profound. This is because if the particle is sufficiently close to the cavity, the double layer surrounding the former is compressed by the latter and the effect of double-layer polarization is affected accordingly. Figure 10c shows that if the particle is positive charged, the induced electric field arising from $D_1 \neq D_2$ drives the particle toward the low-concentration side. On the other hand, if it is negatively charged it is driven toward the high-concentration side by the induced electric field, as seen in Figure 10d. Figure 11 indicates that for small to medium large values of κa the scaled electric force F^*_{e2} increases with increasing κa. This is because the larger the values of κa the higher the surface charge density and the more significant the effect of electrophoresis. However, if κa is sufficiently large, F^*_{e2} declines with increasing κa, and it may become negative if the surface potential is sufficiently high. This is because the direction of the induced electric field arising from type II double-layer polarization is opposite to that of ∇n_0, and the higher the surface potential the stronger the strength of that induced electric field.

Figures 12 and 13 illustrate the variations of the scaled diffusiophoretic velocity U^* as κa and λ (=a/b) vary. According to Figure 12 U^* may have a local maximum and local minimum as κa varies. The smaller the λ (less significant the boundary effect) the easier to observe a local minimum, and the larger the λ the larger the value of κa at which the maximum of U^* occurs. The presence of the local maximum in U^* arises from the competition between the electric force and the hydrodynamic drag acting on the particle; both of them increase with increasing degree of double-layer compression by the cavity. As suggested by Figures 13b−f the larger the κa (thinner double layer) the larger the value of λ necessary to observe the influence of the cavity on the effect of type I double-layer polarization. Figure 14 reveals that the scaled electric force acting on the particle, F^*_{e2}, increases with increasing degree of double-layer compression. It can be inferred that type I double-layer polarization plays the major role here. Similar to the result of Lou and Lee,[23] this is because compression of the double layer yields an increase in the concentration of counterions on the high-concentration side. As seen in Figure 14b the behavior of F^*_{e2} at $|\phi_r| = 5$ is similar to that at $|\phi_r| = 1$ shown in Figure 14a except that F^*_{e2} exhibits a local maximum at $\lambda \cong 0.3$. The presence of the local maximum might due to the fact that the effect of type II double-layer polarization at high potentials is more significant than that at low potentials, and therefore, the effect of double-layer compression by the cavity becomes more complicated. The effect of electrophoresis is important only at small values of λ. On the other hand, as can be inferred from Figure 13, regardless of the value of β the effect of chemiphoresis is important and dominates the motion of the particle at larger values of λ. For example, if $\lambda > 0.5$ the value of U^* in Figure 13a, where $\beta = 0$ (only chemiphoresis is present), is roughly the same as that in Figure 13b, where $\beta = -0.2$ (both chemiphoresis and electrophoresis are present). This implies that the influence of electrophoresis (or β) is relatively unimportant and the movement of the particle is dominated by the chemiphoresis arising mainly from type I double-layer polarization. On the other hand, if $\lambda < 0.5$ $|U^*|$ in Figure 13a is considerably smaller that in Figure 13b, implying that the effect of electrophoresis is more important than that of chemiphoresis. As revealed by Figure 13d the influence of the boundary on the behavior of U^* at high surface potentials is much more complicated than that at low surface potentials. This may arise from the fact that type II double-layer polarization at high surface potentials is more significant than that at low surface potentials. Note that, as shown if Figure 13d, if the surface potential is sufficiently high and κa sufficiently large U^* has two local maxima as λ varies.

The variations of the scaled diffusiophoretic velocity U^* as a function of the position parameter P [=$100m/(b - a)$%] at various combinations of κa and ϕ_r are presented in Figure 15. Here, P measures the degree that the particle deviates from the

center of the cavity or the significance of the boundary effect; the larger the P, the closer the particle to the cavity or the more important the boundary effect. Figure 15 indicates that U^* has a local maximum as P varies, which occurs at a point close to the cavity surface. This is because the concentration of counterions on the high-concentration side of the particle is higher than that on the low-concentration side. If P is large the compression of the double layer by the cavity leads to a further increase in the degree of that type I double-layer polarization and, therefore, an increase in the electric force acting on the particle. On the other hand, a larger P also leads to a greater hydrodynamic drag arising from the presence of the cavity. This phenomenon is enhanced as the surface potential and/or value of P are raised. The diffusiophoretic flow, which flows from the high-concentration side of the particle within the double layer to the low-concentration side, drives the particle toward the low-concentration side is also enhanced as the double layer on the high-concentration side is compressed by the cavity. This is illustrated in Figure 15a, which shows the variations of the relevant scaled forces as a function of P. Recall that in the first subproblem the particle moves at a constant velocity U in the absence of ∇n_0. In this case, the absolute value of the scaled hydrodynamic force, $|F^*_{d1}|$, increases with increasing P on account of the nonslip condition on the surfaces of the particle and the cavity, as seen in Figure 16a. In addition, $|F^*_{e1}| = 0$, implying that the relaxation effect is negligible at low surface potential and/or small Pe. The latter is consistent with that pointed out by Masliyah and Bhattacharjee.[33] In the second subproblem ∇n_0 is applied but the particle remains fixed in the space. In this case, the scaled hydrodynamic force F^*_{d2} is negative because the diffusiophoretic flow (chemiphoretic in this case) is from the high-concentration side to the low-concentration side along the particle surface, as shown in Figure 7a. The scaled electric force F^*_{e2} is seen to have a local maximum as P varies. This is because compression of the double layer by the cavity leads to an increase in not only the degree of type I double-layer polarization but also the repulsive force between coions and the particle. Note that as $P \rightarrow 100\%$, the net scaled electric force ($F^*_{e1} + F^*_{e2}$) is small, the movement of the particle is dominated by F^*_{d2} (i.e., by chemiphoretic flow in this case), and it moves toward the low concentration side. As seen in Figure 16b if the surface potential is high, $F^*_{e1} \neq 0$ and the direction of this force is opposite to that of the movement of the particle. In this case, the attractive force between the particle and counterions becomes strong, and therefore, the relaxation effect becomes significant. However, because Pe (=0.26) is small, $|F^*_{e1}|$ is relatively small compared to other scaled forces.

The variations of the scaled diffusiophoretic velocity U^* as a function of the scaled surface potential ϕ_r at various values of the electric Peclet number Pe are illustrated in Figure 17. As seen, if ϕ_r is low the influence of Pe on U^* is unimportant, that is, the convective terms on the right-hand side of eqs 9 and 10 are negligible, implying that the relaxation effect is insignificant. In addition, U^* decreases with increasing Pe. Conclusions similar to these were also made in the electrophoresis of a particle driven by an applied electric field.[30,33,42] If the diffusivity of counterions is small, the relaxation effect becomes significant, and because Pe $\propto 1/D$, the larger the Pe the slower the velocity of the particle.

Conclusions

In summary, the boundary effect on the diffusiophoretic behavior of a particle is analyzed by considering a charged spherical particle at an arbitrary position in an uncharged spherical cavity under conditions of an arbitrary level of surface potential and double-layer thickness. We show that two types of double-layer polarization are present: that due to the uneven distribution of counterions inside the double layer and that due to accumulation of coions near the outer boundary of the double layer. The former drives the particle toward the high-concentration side of the applied concentration gradient and the latter, which is significant if the surface potential is high, drives the particle toward the low concentration side. The direction of diffusiophoresis depends upon which effect is more significant.

The unbalanced amount of counterions in the double layer on the high- and low-concentration sides of the particle arising from application of the concentration gradient yields a diffusion flow. If the difference between the diffusivity of counterions and that of coions is large, electroosmotic flow dominates; if it is small, chemiphoresis flow dominates. If the diffusivity of counterions and that of coions are the same and the boundary effect is relatively unimportant, the scaled diffusiophoretic velocity of the particle has a local maximum as the level of surface potential varies, and the thinner the double layer the larger the local maximum. On the other hand, if the boundary effect is important, the local maximum shows a maximum as the thickness of the double layer varies.

The scaled diffusiophoretic velocity may have a local maximum and local minimum as the thickness of the double layer varies. The less significant the boundary effect the easier it is to observe a local minimum. If the boundary effect is insignificant, electrophoresis dominates; if it is significant, then chemiphoresis dominates. The scaled diffusiophoretic velocity has a local maximum as the position of the particle varies; the local maximum occurs at a point close to the cavity surface. The influence of the boundary on the behavior of the particle at high surface potentials is much more complicated than that at low surface potentials.

If the surface potential is low, the influence of the electric Peclet number on the diffusiophoretic velocity is unimportant, implying that the relaxation effect is insignificant. If the diffusivity of counterions is small, the relaxation effect becomes significant, and the larger the electric Peclet number the slower the scaled diffusiophoretic velocity.

Acknowledgment. This work was supported by the National Science Council of the Republic of China.

LA803334A

(42) Henry, D. C. *Proc. R. Soc. London* **1931**, *133A*, 106.